Supplementary Information for

Photoconductive focal plane array based on HgTe nanocrystals for fast and cost-effective short-wave infrared photodetection

Charlie Gréboval[1], David Darson[2], Victor Parahyba[3], Claire Abadie[4], Vincent Noguier[3], Simon Ferré[3], Eva Izquierdo[1], Adrien Khalili[1], Yoann Prado[1], Pierre Potet[4], Emmanuel Lhuillier[1*]

[1] Sorbonne Université, CNRS, Institut des NanoSciences de Paris, INSP, F-75005 Paris, France.
[2] Laboratoire de Physique de l'Ecole normale supérieure, ENS, Université PSL, CNRS, Sorbonne Université, Université Paris-Diderot, Sorbonne Paris Cité, Paris, France.
[3] New Imaging Technologies SA, 1 impasse de la Noisette 91370 Verrières le Buisson, France.
[4] ONERA - The French Aerospace Lab, 6, chemin de la Vauve aux Granges, BP 80100, 91123 Palaiseau, France.

*To whom correspondence should be sent: el@insp.upmc.fr

Table of content

1. Material characterization

As NCs are processed under ink form we observe a systematic shift of the band edge by ≈500 cm^{-1}. In addition, the C-H peak (doublet at 2851 and 2919 cm^{-1},) decreases in magnitude, consistent with the reduction of the ligand length from C12 to C2. The small amine peak (at 3300 cm^{-1}) that result from left over olyelamine, is replaced by a broad and intense peak that we attribute the to the O-H bond coming from mercaptoethanol.

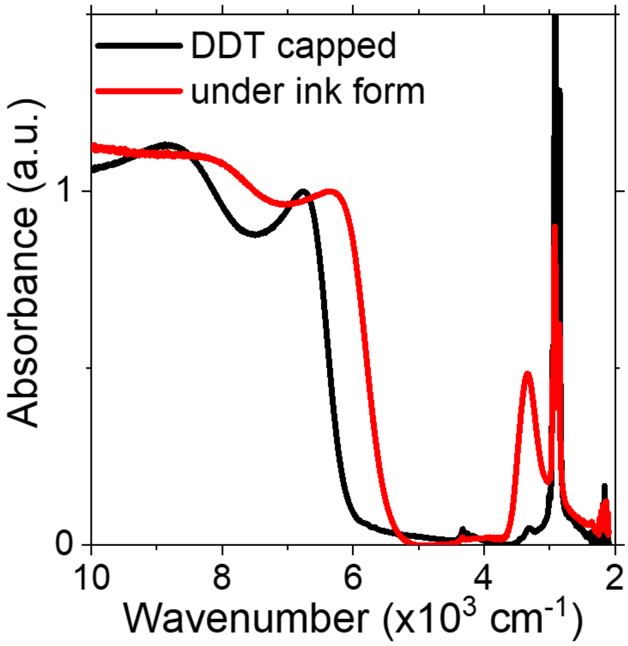

***Figure S 1 Absorbance of the HgTe NCs** capped with DDT ligands (as it is et the end of synthesis) and under ink form.*

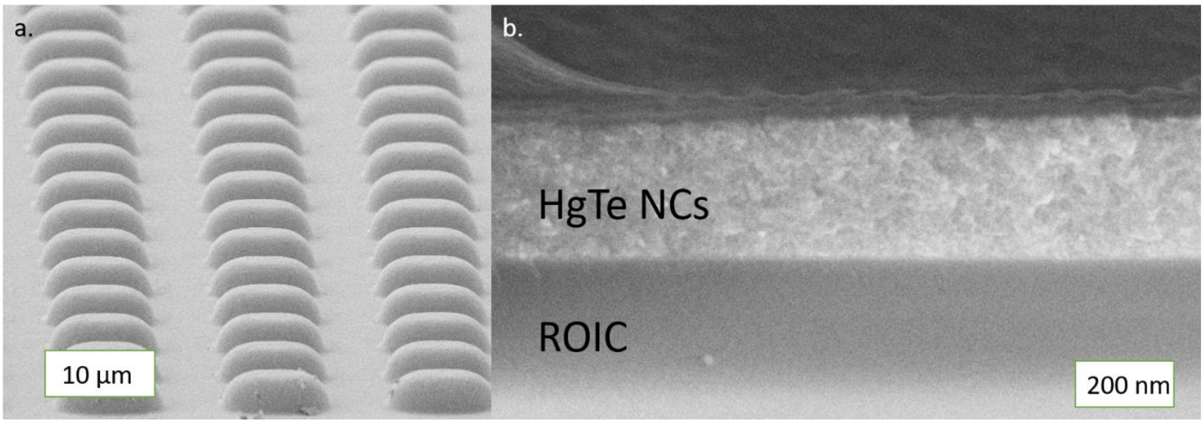

Figure S 2 SEM image of HgTe NCs film deposited on a ROIC, top view (a.) and a cross section view (b).

2. Electromagnetic and electrostatic simulations

2.1. Spectroscopic ellipsometry

The complex optical index of HgTe NC thin film[1] has been determined by spectroscopic ellipsometry and is shown in Figure S 3. This index is later used as input for electromagnetic simulation shown as Figure 2.

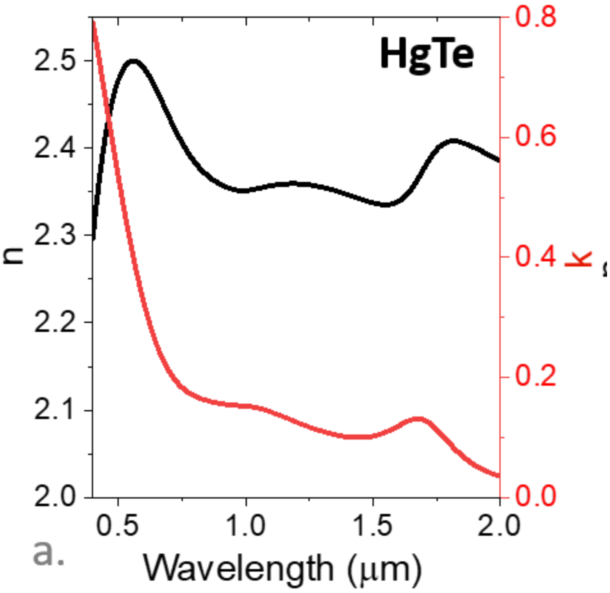

Figure S 3 a. Refractive index and extinction coefficient for HgTe NC film.

2.2. Electrostatic simulation

Figure S 4 shows the electrostatic field and the associated current density map as two pixels of the ROIC are polarized with different biases (0 and 1 V respectively)

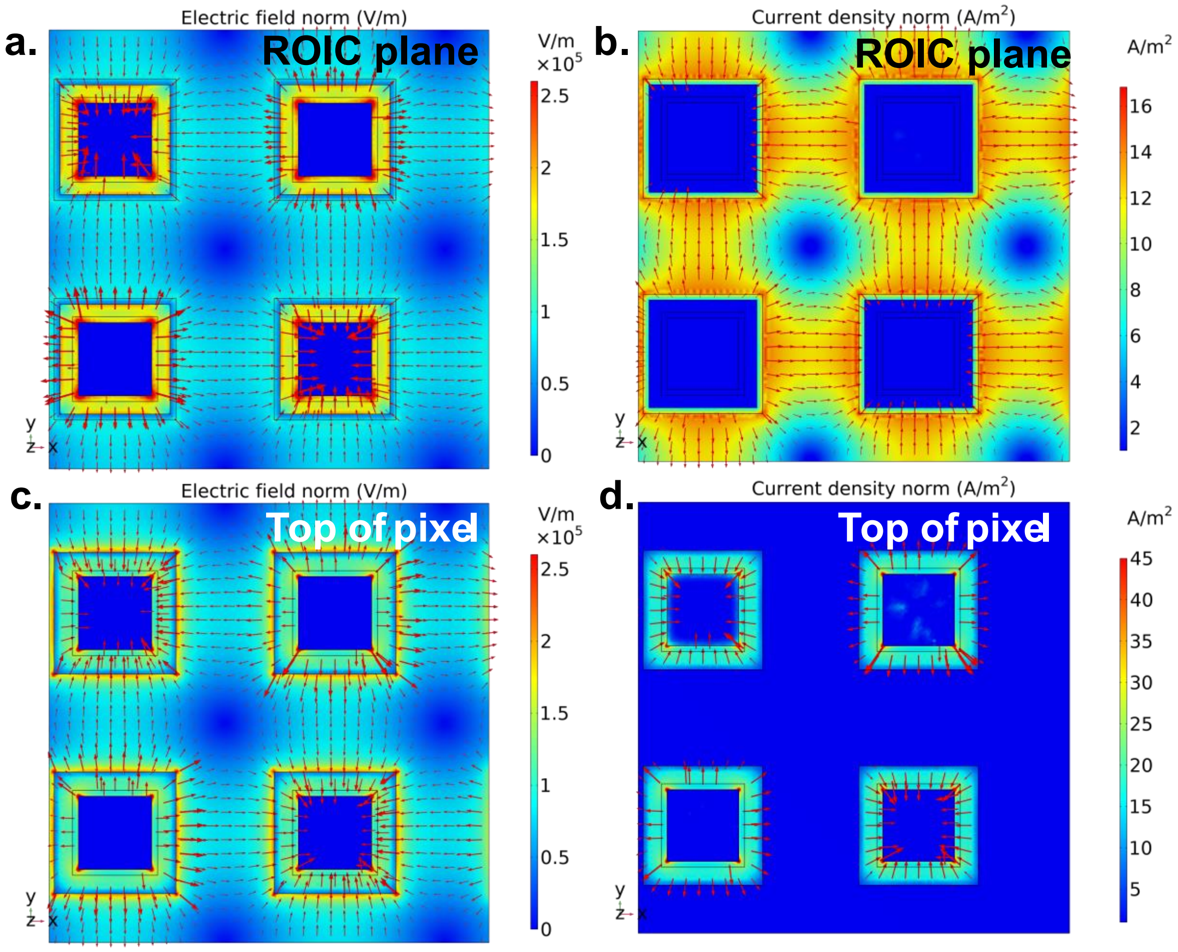

Figure S 4 Comsol electrostatic simulations*. Simulated Electric potential of the ROIC which are biased to 0 and 1 V alternatively, for the bottom plane of the ROIC (a.) and for the top plane of the pixel (c.). The norm of the electric field is represented by the color map while the direction by the arrows. Simulated current density of the ROIC with periodic boundary conditions in the bottom plane of the ROIC (b.) and in the top pixel plane (d.). The norm of the current density is represented by the color map while the direction by the arrows.*

3. Peltier cooled setup

The two stage Peltier enables operation between -40 °C and room temperature while the temperature of the chip is stabilized thanks to a PID regulation. An image of the camera is provided in **Figure S 5**

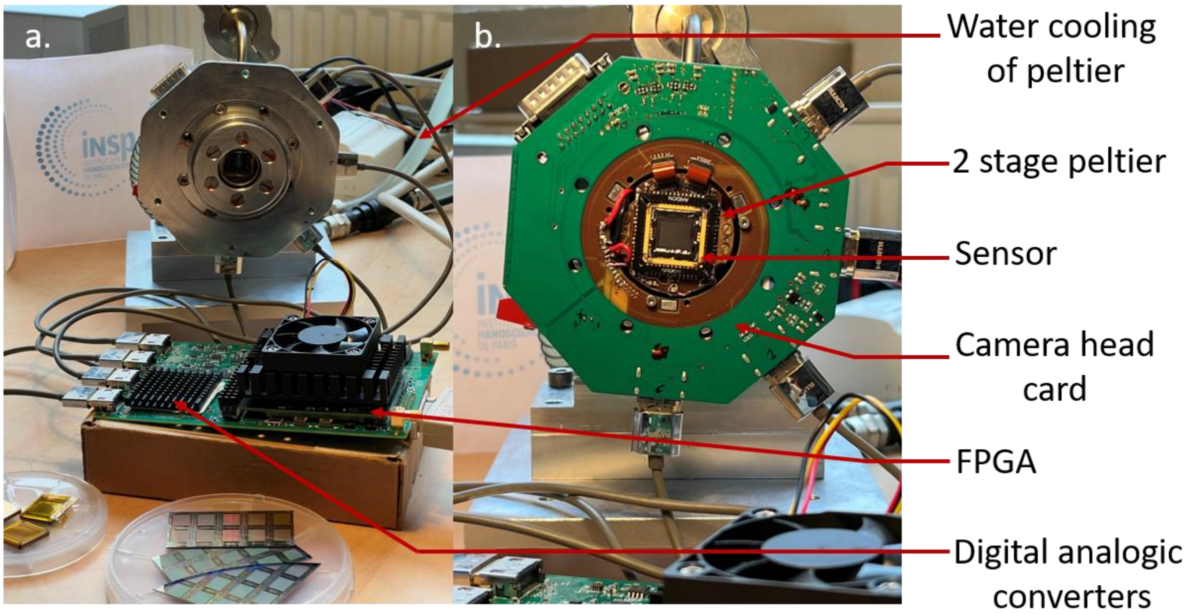

Figure S 5 Picture of the Peltier-cooled camera setup. *a. The head of the camera is on the top of the picture and in the foreground there is the electronic card (Digital Analogic Converters, FPGA, etc.). b. Zoom on the head of the camera when the window is removed showing the ROIC mounted on the camera.*

4. EQE determination

To determine the EQE of the FPA, the sensor is illuminated by an LED at a given wavelength (940 and 1570 nm) while the incident power is tuned. From the histogram of intensity, we extract an average value, which is then plotted as a function of the incident power. The data are then fitted using a linear fit (to exclude the saturated regime) and the slope is compared to the InGaAs one, that is assumed to correspond to an absolute EQE of 90%, see **Figure S 6** and **Figure S 7**

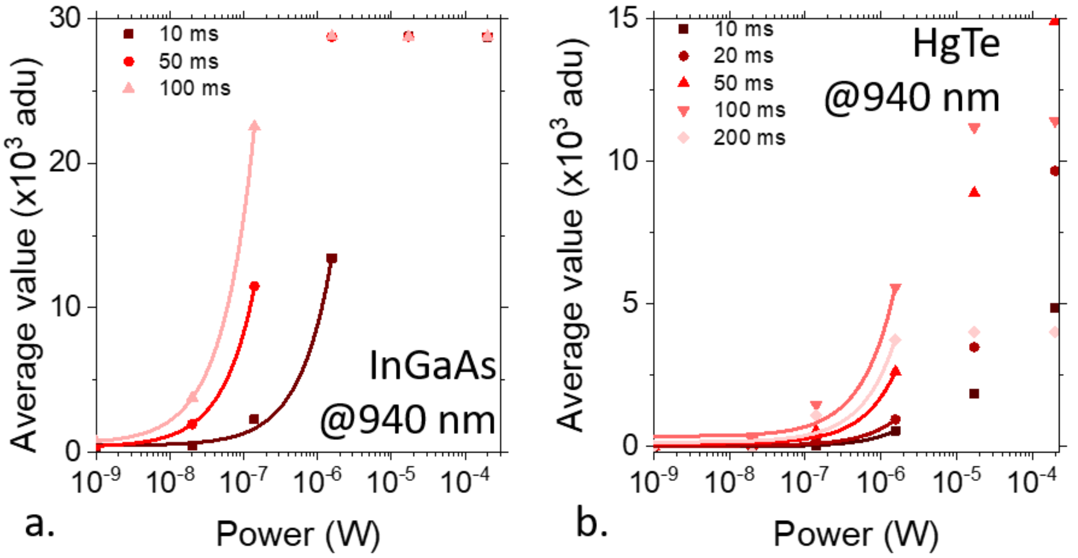

***Figure S 6 Comparison of the InGaAs and HgTe NC based sensor**. Evolution of the average value of a homogeneously illuminated image by a LED at 940 nm as a function of the power for various exposure times. The solid lines are linear fits of the points. Part a is for InGaAs and part b for the Hgte NC based FPA.*

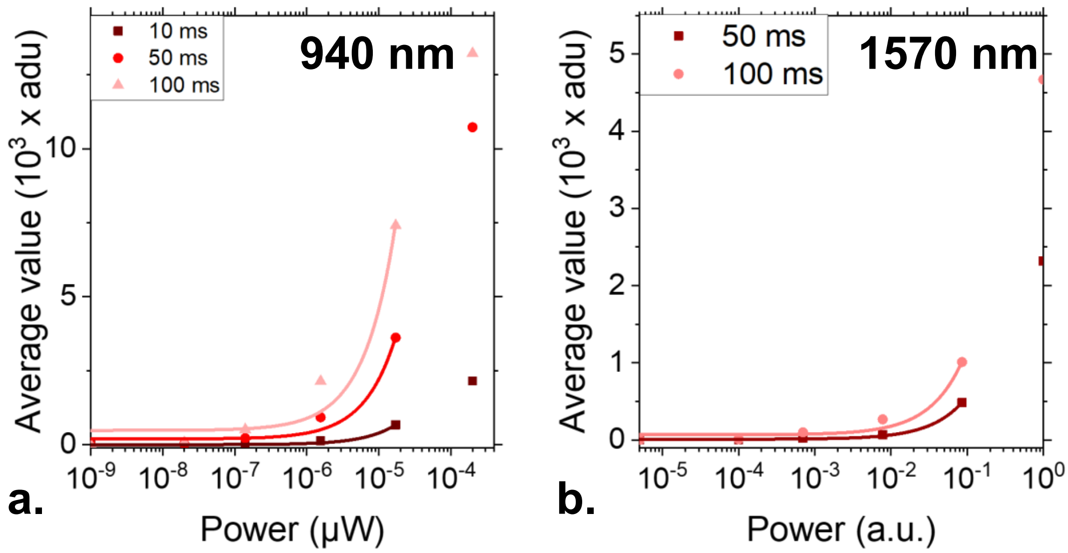

***Figure S 7 EQE for the HgTe NC based FPA.** a. Evolution of the average value of a homogeneously illuminated image by a LED at 940 nm as a function of the power for various exposure times. The solid lines are linear fits of the points. b. Evolution of the average value of a homogeneously illuminated image by light at 1570 nm as a function of the power for various exposure times. The solid lines are linear fits of the data points.*

5. High frame rate imaging

Figure S 8 and video S4 shows the high frame rate imaging of a chopper wheel, while only half of the pixel are used.

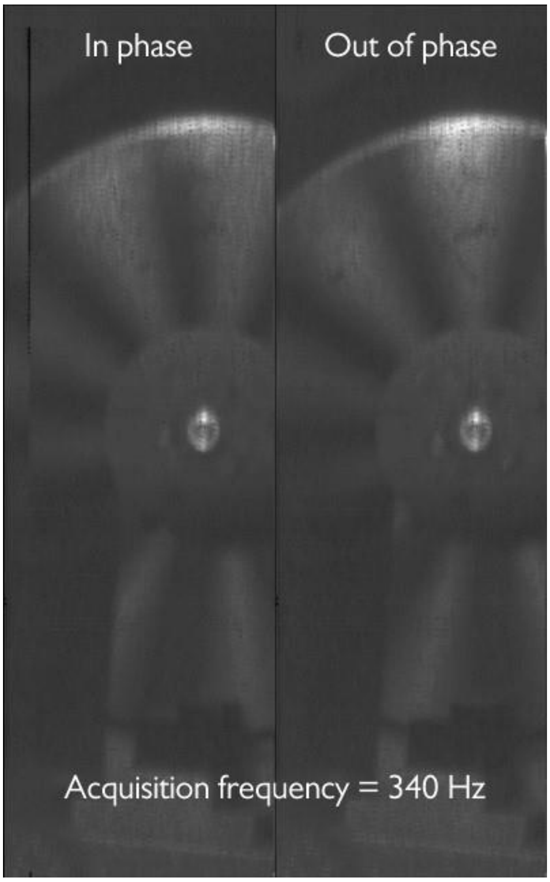

Figure S 8 Image extracted from video S4 *showing a chopper wheel imaged at 340 Hz. On the left the chopper frequency matches the acquisition frequency while on the right the chopper frequency is detuned. Exposure time is set to 1000 µs and the camera temperature to -32 °C. The region of interest is reduced to 640 x 200 pixels to reach such framerate.*

6. Non homogeneity correction

Figure S 9 illustrates the procedure to correct the image. Examples of raw image are shown in **Figure S 9**a (homogeneous illumination – illumination through a diffusive medium) and e (for a complex scene). From this picture, we offset the image obtained in the dark condition (i.e., dark current correction, and assuming that the offset level at 0 s exposure time is contained on the dark condition image), and we then divide by the one obtained under homogeneous illumination (i.e., gain correction), leading to a corrected image. **Figure S 9**b and d show how the histogram of intensity gets corrected by this procedure. The histogram of the intensity is shifted (dark current correction) and gets narrower (gain correction). For sake of illustration this procedure is shown with the picture of a scene, see **Figure S 9**e. and f. Basically, the raw image from part a is removed from part e and then we divide the result by image c to obtain image f.

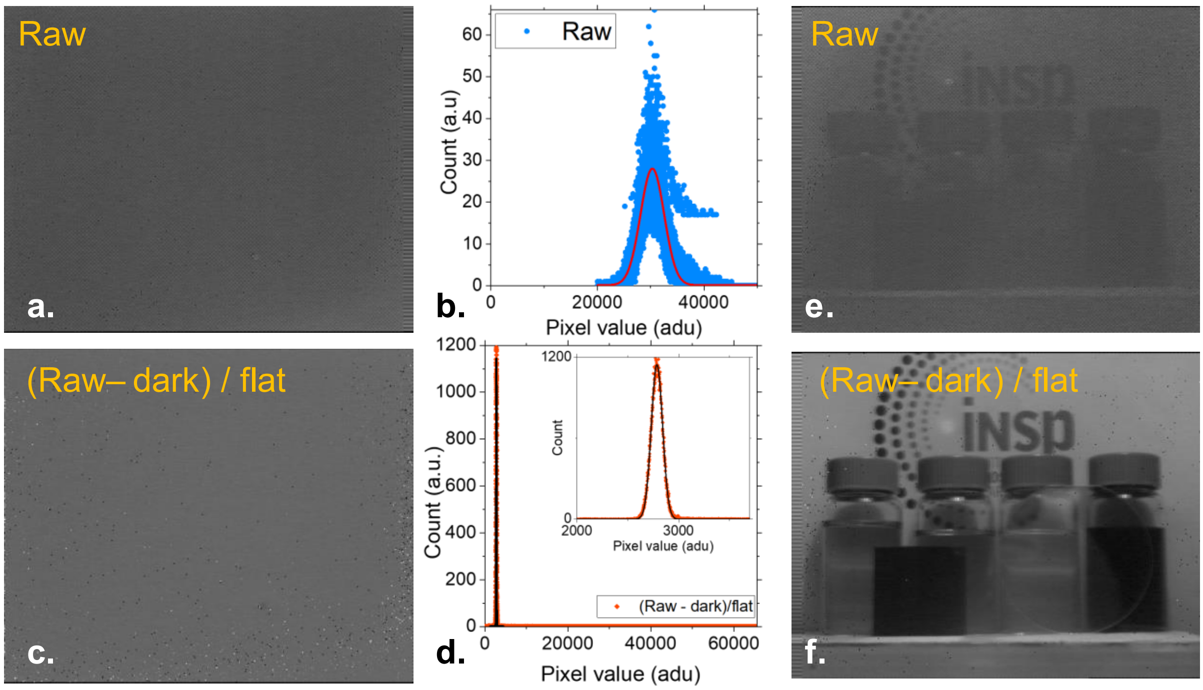

***Figure S 9 Pixel homogeneity**. a. Picture under homogeneous lighting at 940 nm and 200 µW of power taken with an exposure time of 50 ms and a temperature of -30 °C. b. Histogram of the image shown in (a.) fitted with a gaussian model showing a standard deviation of 2200 adu and an integrated count of 156000. c. Same picture as in (a.) after subtraction of the dark signal and a normalization by a flat image taken in the same conditions. d. Histogram of the image shown in (c.) fitted with a gaussian model showing a standard deviation of 50 adu and an integrated count of 160000. Inset shows a zoom on the gaussian that appears as a line on the graph. e. Raw picture of a scene illuminated by a tungsten lamp before correction. f. Same image as (e.) after offset/flat correction.*

7. Spectral response

Figure S 10 shows the same scene as Figure 5, while some band pass filters have been added. Each filter has a bandwidth of 50 nm.

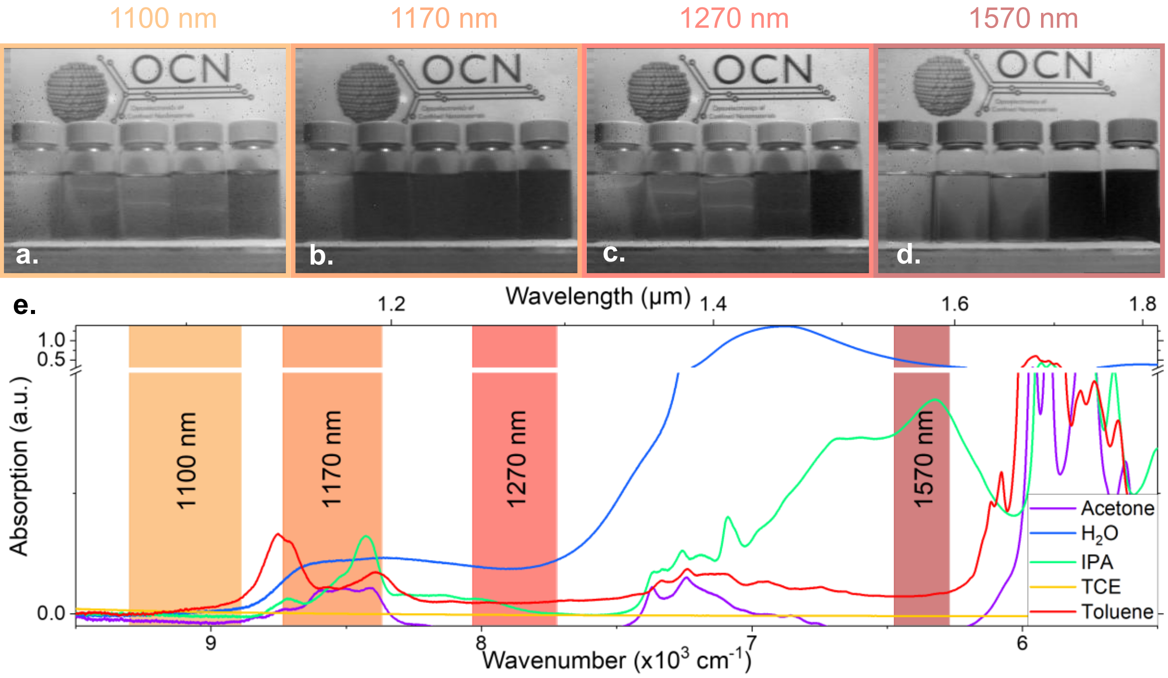

Figure S 10 Imaging over the SWIR region of different vials containing solvents that are transparent in the visible*. From left to right, vials containing tetrachloroethylene, toluene, acetone, isopropyl alcohol and water. a., b., c. and d. have been taken using different band pass filters which are represented by vertical rectangles on (e.) e. Absorption spectra of the different solvents imaged in the pictures a-d. with the transmission bands of the different filters.*

Figure S 11 are two images respectively extracted from Video S2 and S3. It in particular shows the lack of memory effect.

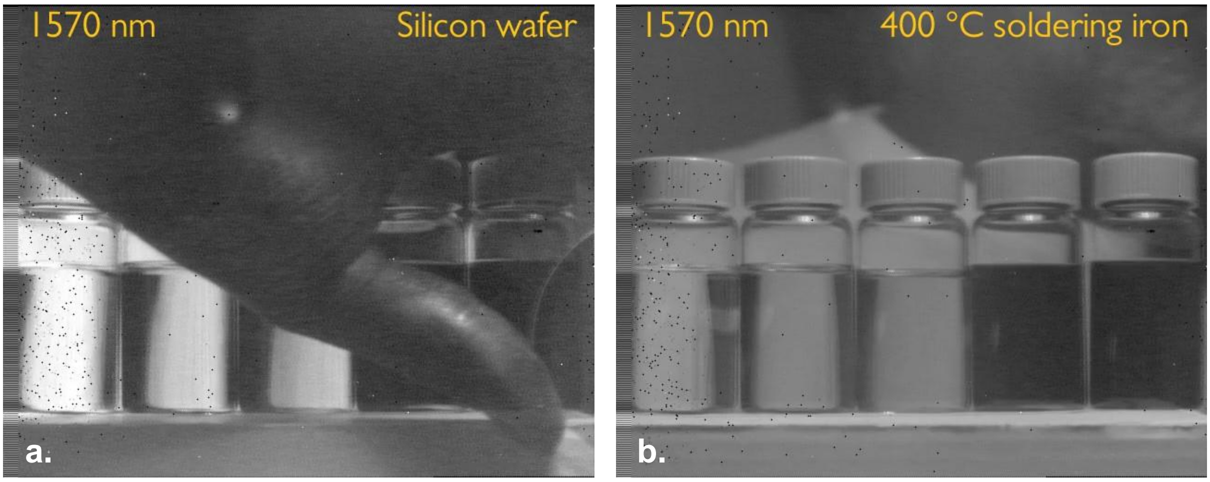

***Figure S 11 Images extracted from the S2 (left) and S3 (right) videos** showing a scene with 5 solvents (from left to right: TCE, toluene, acetone, IPA, water) in front of which are passed (a.) some substrates (silicon and ITO on glass) and (b.) a soldering iron at 400 °C.*

8. REFERENCES

1 P. Rastogi, A. Chu, T. H. Dang, Y. Prado, C. Gréboval, J. Qu, C. Dabard, A. Khalili, E. Dandeu, B. Fix, X. Z. Xu, S. Ithurria, G. Vincent, B. Gallas and E. Lhuillier, *Adv. Opt. Mater.*, 2021, **9**, 2002066.